Comparison of Diffusion of *N*,*N*-Dimethylaniline and *N*,*N*-Dioctadecylaniline in a Low-Density Polyethylene Film. Activation Energies and Detection of Two Diffusion Pathways†

John A. Taraszka‡ and Richard G. Weiss*

Department of Chemistry, Georgetown University, Washington, D.C. 20057-1227

Received October 28, 1996; Revised Manuscript Received January 21, 1997⊗

ABSTRACT: The diffusion of *N*,*N*-dimethylaniline and *N*,*N*-dioctadecylaniline from a low-density polyethylene film into 2 N hydrochloric acid was measured in real-time at various temperatures by fluorescence spectroscopy. Diffusion coefficients (*D*) were obtained from each data set by a best fit to a series expansion of the integrated form of Fick's second law for diffusion through a film. The activation energies for diffusion (E_D) were calculated from the *D* values in a temperature range above the glass transition and below the melting transition assuming Arrhenius behavior. As expected, *N*,*N*-dioctadecylaniline diffusion was slower than that of *N*,*N*-dimethylaniline at one temperature. Somewhat surprisingly, good fits of the *N*,*N*-dioctadecylaniline data sets to the series expansion require a model with *two* concurrent, independent diffusion processes; two diffusion coefficients at each temperature and two values of E_D, 16 ± 4 and 4 ± 1 kcal/mol, are calculated. The significantly higher activation energy, similar in magnitude to the single E_D of *N*,*N*-dimethylaniline, 15.7 ± 0.4 kcal/mol, is associated with the more rapid diffusional component. The data are discussed in terms of the type of sites occupied by the anilines and the influence of the two molecules on their local environments.

Introduction

There are literally hundreds of "polyethylenes," each differing from the others in degree of crystallinity, thermal history, mechanical history, number and type of chain branches, and degree and types of unsaturation.[1] The noncrystalline regions consist of an amorphous part (in which chains are disordered and may be entangled and branched) and an interfacial part along the boundaries between microcrystallites and amorphous domains (in which chains are oriented in a more or less parallel fashion but do not contribute to the heat of melting[2]). To complicate matters further, the interfacial part may have separate regions that resemble more the crystal or the amorphous organizations.[3]

To understand better the *dynamic* nature of polyethylene, we have measured the diffusion coefficients (*D*) and activation energies (E_D) for one or more *N*,*N*-dialkylanilines (DAA) in unstretched and stretched, native and modified films[4,5] that are well-characterized.[6] Among the films employed is NDLDPE, 42% crystalline in its unstretched, native state. Its other physical characteristics are included in Table 1.[6]

It is known that molecules like DAA are unable to enter the crystalline regions of polyethylene under the conditions of our experiments.[7] There are, however, at least two families of polyethylene sites at which guest molecules can reside,[8] in the amorphous and interfacial regions.[4,5,7,9] If the physical processes associated with the motions leading to and from the two site types are sufficiently different, it should be possible to distinguish them kinetically by detecting two diffusion coefficients for one species in one film.

To the best of our knowledge, a bimodal distribution for a diffusing guest molecule in polyethylene has not been reported previously. In our own work with low-density polyethylenes (i.e., ≤50% crystallinity), increasing the alkyl chain length in a series of DAA from methyl (DMA, molecular mass 121) to butyl (DBA, molecular mass 205) resulted in diffusion that could be described precisely by a single diffusion coefficient[5a] using a truncated series expansion of the integrated form of Fick's second law.[10]

Table 1. Some Properties of NDLDPE Films[6]

density: 0.918 g cm^{-3}
thickness: 70 μm
degree of crystallinity: 42%
interfacial region: 3%
melting temperature: 116 °C
partition coefficient for DMA between film and methanol at 25 °C: 0.30 ± 0.01
CH_3 groups per 1000 CH_2 groups: 25
C=C groups per 1000 CH_2 groups: 0.49
C=C groups per 1000 CH_2 groups inaccessible to 17 wt % Br_2 in $CHCl_3$: ca. 0

Here, values of *D* and E_D are reported for the diffusion of DMA and a much larger molecule, *N*,*N*-dioctadecylaniline (DODA, molecular mass 597) in NDLDPE. Although diffusion of DMA can be described, as expected,[11] by a single diffusion constant, that of DODA cannot be. A model with two distinctly different diffusion coefficients can be invoked to fit the DODA data well. Accordingly, increasing the molecular mass and size of the guest molecule permits differences between the two (principal) DAA diffusion modes predicted by the model to become detectable. The corresponding E_D values suggest possible origins of each component.

Experimental Section

Materials. *N*,*N*-Dimethylaniline (99%, Aldrich) was distilled under vacuum and stored under nitrogen away from light. The polyethylene film from Dupont of Canada, designated NDLDPE, was 70 μm thick (Table 1[6]). Prior to being used, film pieces were immersed in batches of chloroform for several hours to remove antioxidants and plasticizers. Methanol (Burdick-Jackson Chromopure), *n*-pentane (Fisher, spectro grade), hexadecane (Aldrich, 99%), and hexane and ethyl acetate (Fisher, HPLC grade) were used as received.

N,*N*-Dioctadecylaniline was synthesized by repeated reaction of aniline with octadecanoyl chloride followed by reduction with $LiAlH_4$. In the final step, a mixture of *N*-octadecyl-*N*-

† Dedicated to Waldemar Adam on the occasion of his 60th birthday.

‡ John T. Adams Undergraduate Research Fellowship recipient.

⊗ Abstract published in *Advance ACS Abstracts,* April 1, 1997.

S0024-9297(96)01592-6 CCC: $14.00 © 1997 American Chemical Society

phenyloctadecanamide (mp 55.3−59.1 m, °C; 400 mg, 0.656 mmol), 25 mL of dried THF, and $LiAlH_4$ (74.7 mg, 1.97 mmol) were stirred and refluxed at 80 °C for 2 h under a dry atmosphere. Excess $LiAlH_4$ was destroyed by adding ethyl acetate and distilled water. The solid was filtered under vacuum and rinsed with copious amounts of ether. The ether and THF layers were recombined and evaporated. The residue was dissolved in a minimal amount of hexane and extracted thrice with distilled water. The hexane layer was dried over anhydrous K_2CO_3 and evaporated under vacuum. The crude residue was purified by column chromatography (silica gel, 98/2 hexane/ethyl acetate) to yield 215 mg of product, mp 40.8−43.0 °C (lit[12] mp 52−53 °C), that was 99.3% pure by HPLC analysis.

FT-IR (KBr, cm^{-1}): 2916 and 2849 (C−H stretch); 1607 (aromatic).

^{1}H-NMR ($CDCl_3$/TMS): 7.21−7.16 (aromatic, m, 2H), 6.64−6.61 (aromatic, m, 3H), 3.27−3.21 (N−**CH_2**, t, 4H, J = 7.7 Hz), 1.56 (N−CH_2−**CH_2**, broad s, 4H), 1.26 (various CH_2 groups, broad s, 60H), 0.91−0.86 (CH_3, t, 6H, J = 6.6 Hz) ppm. GC/MS: calculated M/z 597; obtained M/z 597 (1.4%); (M + 1)/z (3.9%), (M + 2)/z (1.9%).

Instrumentation. UV−vis absorption spectra were recorded on a Perkin-Elmer Lambda 6 spectrophotometer in hexane or hexadecane. Spectra of films were obtained between two quartz plates. FT-IR spectra were obtained with a MIDAC FT-IR using Spectra Calc version 2.21 software. Solids were prepared as KBr pellets. A blank KBr pellet was used for background correction. Mass spectra were obtained at 70 eV on a Shimadzu QP 5000 direct inlet quadrupole mass spectrometer by Dr. Donald Weber. A Bruker 270 MHz FT-NMR spectrometer with an Apple Quadra 950 computer was used to obtain proton NMR spectra.

HPLC chromatograms were recorded on a Waters 6000A solvent delivery system and a Waters Model 440 UV absorbance detector (254 nm) in conjunction with an Alltech 25 cm analytical silica gel column. A Spectra-Physics Autolab Minigrator was used to integrate the data. The eluting solvents were either 12/88 or 5/95 ethyl acetate/hexane.

Emission and excitation spectra and time-dependent emission intensities were obtained on a Spex 111 Fluorolog fluorimeter with an Osram 150 W/XBO high-pressure Xe lamp and 1.25 mm slits. Samples were thermostated (±0.3 °C) using a VWR 1140 circulating constant temperature bath, and temperatures were monitored using a calibrated thermistor that was in contact with the sample cuvette. Analyses of fluorescence intensity data and fits to model equations employed the Windows versions of Quattro Pro and Origin 3.5.

Procedures for Obtaining Diffusional Data.[4d,13] Prior to being doped, a 1 × 2−3 cm piece of NDLDPE film was immersed in four aliquots of chloroform for 6 h each (to remove plasticizers and antioxidants) and air dried. The "clean" film was mounted taut on a glass yoke[4c] and immersed in a 4.7 × 10^{-3} M pentane solution of DODA or a 2 × 10^{-2} M methanol solution of DMA for 2−2.5 h (i.e., until an embibed concentration of ca. 10^{-3} M had been attained). In experiments with ca. 10^{-1} M initial DMA in a film, the methanolic doping solution contained 10^{-1} M DMA and the film immersion time was ca. 8 h. Initial film concentrations within a film were determined periodically by absorption spectroscopy using the Beer−Lambert law and molar extinction coefficients in hexadecane: for DMA, λ_{max} 298 nm (ϵ_{max} 14 730 L mol^{-1} cm^{-1}); for DODA, λ_{max} 259 nm (ϵ_{max} 12 900 L mol^{-1} cm^{-1}). The film was removed from the bath, washed with methanol to remove any surface-occluded DAA, dried under a stream of nitrogen, and rapidly placed in a thermostatted quartz cuvette containing 3 mL of 2 N hydrochloric acid (prepared from distilled water and concentrated HCl) that was inside the sample compartment of the fluorimeter. Immediately, the intensity of fluorescence was measured at a right-angle (front-face) configuration as a function of time until the rate of change in intensity was small. For DMA, λ_{ex} = 300 nm and λ_{em} = 350 nm; for DODA, λ_{ex} = 303 nm and λ_{em} = 335 nm.

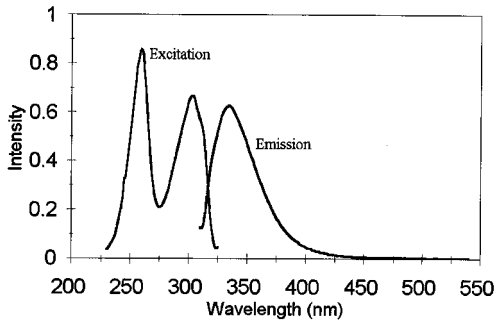

Figure 1. Emission (λ_{ex} = 303 nm) and excitation (λ_{em} = 335 nm) spectra of 2.6 × 10^{-5} M DODA in hexane at room temperature.

Results

Steady State Emission and Excitation Spectra. Emission and excitation spectra of *N*,*N*-dioctadecylaniline in hexane, a solvent whose polarity is similar to that of polyethylene, appear in Figure 1. Emission and excitation spectra of DMA have been reported previously.[5a] In 2 N HCl, the absorption (or excitation) maximum suffers a large hypsochromic shift and the intensity of emission is decreased drastically.

Time-Dependent Emission Spectra. DMA and DODA were excited at wavelengths at which the NDLDPE film does not absorb. Due to the heterogeneous nature of the films, emission intensities were found to vary depending on the spot on the surface being excited. Therefore, each film was not moved during the duration of a run. However, runs in which fluorescence intensities are measured at different parts of the same piece of film led to reproducible values of D. In fact, the same piece of film can be (and usually is) employed for several months of diffusional experiments without suffering detectable changes in its properties.

Emission intensity decay curves like those in Figure 2 were measured starting as close to real time = 0 (i.e., when a doped film was placed in the aqueous acid) as possible. Practically, the experimental manipulations require a minimum of 20 s before data are recorded. Intensities at time = 0, I_0, were estimated using eq 1, a

$$I_t = I_0 - (I_0 - I_\infty)(4/l)(D/\pi)^{1/2}t^{1/2} \qquad (1)$$

modified form of the "early time" formulation of Fick's second law,[11a] by extrapolating the slope of the linear region of I_t vs $t^{1/2}$ to its y-intercept. In eq 1, I_t is the fluorescence intensity at time equals t and l is the thickness of the film. I_∞ is taken to be the intensity when changes of <1% of the intermediate value occur during a 30 min period. At 25, 35, and 45 °C, I_∞ was reached after 15, 11, and 8 h, respectively, for DODA and ca. 65, 50, and 35 min for DMA. Note that I_0 refers to the value at "instrumental" time = 0 rather than the measured value; see, for example, Figure 3.

An exception to this procedure was adopted in experiments with initial concentrations of ca. 10^{-1} M DMA. There, the intensity data could not be fit successfully at early times to eq 1 (or other models tried). Analyses are based on data collected after 500, 250, and 100 s at 25, 35, and 45 °C, respectively.

Using the calculated I_0 values, plots of $I_{rel} = (I_t - I_\infty)/(I_0 - I_\infty)$ vs time were fit to a series expansion form of Fick's second law that was truncated to the first eight terms (eq 2). In other work, we have found that adequate fits can be obtained with as few as three terms[5a] and they are not improved greatly by as many

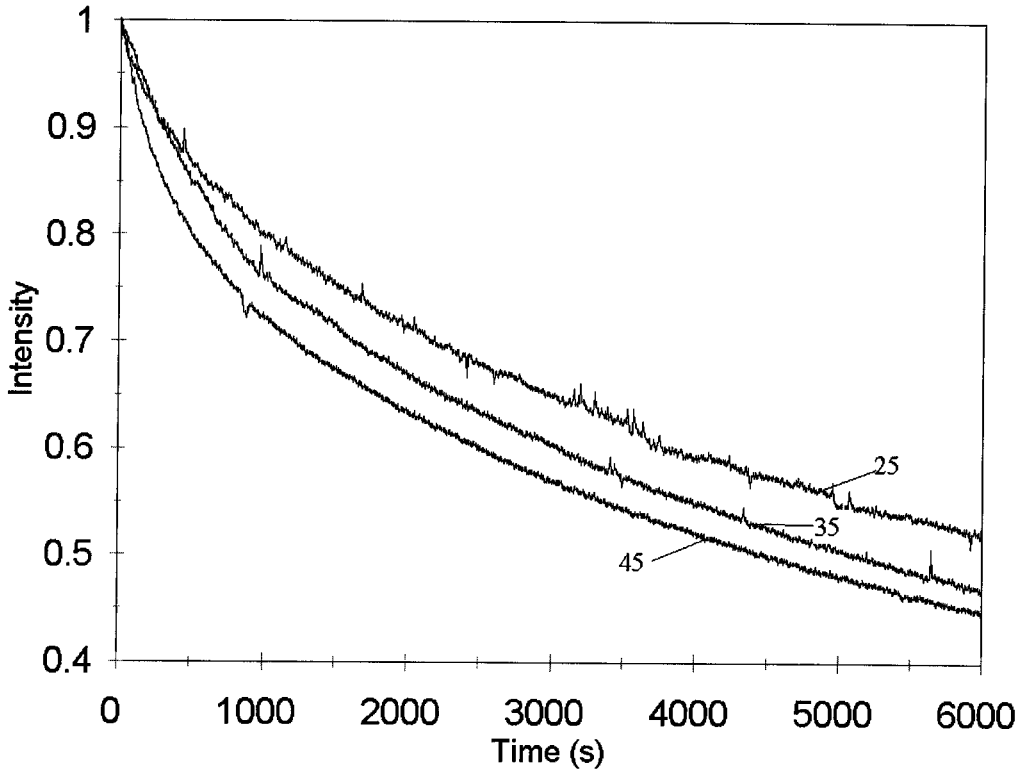

Figure 2. Plots of I_t (normalized to I_0) vs t for DODA in NDLDPE after immersion in 2 N HCl at 25, 35, and 45 °C.

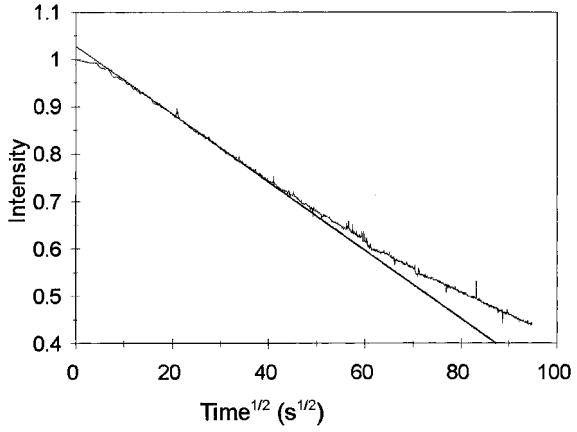

Figure 3. Plot of I_t vs $t^{1/2}$ for DODA in NDLDPE at 25 °C after immersion in 2 N HCl. The slope is calculated between 225 and 630 s.

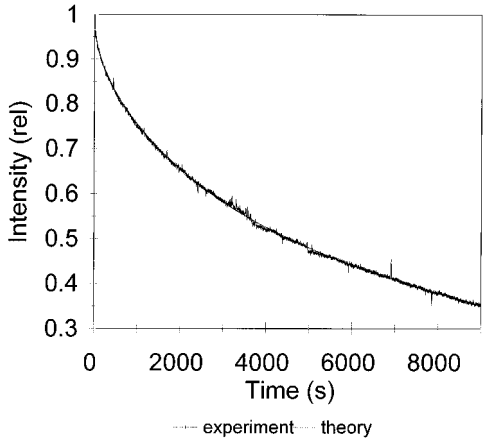

Figure 4. Plot of I_{rel} vs t for diffusion of DODA in NDLDPE at 25 °C (jagged line) and the best fit to eq 3 (smooth line). Congruence of the two makes the smooth line nearly undetectable.

as 50 terms.[6] At early times, where additional terms aid curve fitting most, our data is least reliable due to the experimental methods described in the Experimental Section. For DODA, the best fits to data sets were clearly unsatisfactory, and a double summation expression involving two diffusion coefficients and a weighting factor (where $0 \leq C \leq 1$) was employed (eq 3).

$$I_{rel} = \sum \frac{8}{(2n+1)^2\pi^2} e^{-[D(2n+1)^2\pi^2 t/l^2]} \quad (2)$$

$$I_{rel} = C\sum \frac{8}{(2n+1)^2\pi^2} e^{-[D_1(2n+1)^2\pi^2 t/l^2]} + (1-C)\sum \frac{8}{(2n+1)^2\pi^2} e^{-[D_2(2n+1)^2\pi^2 t/l^2]} \quad (3)$$

In eq 2, the only floating variable is D. In equation 3, D_1, D_2, and C were varied simultaneously to obtain a best fit. An example is shown in Figure 4. The fits to data of runs involving ca. 10^{-3} M initial DAA concentrations are excellent in all cases as judged by χ^2 values that were $\leq 1.2 \times 10^{-4}$ (Tables 2 and 3). In runs with 10^{-1} M initial concentrations of DMA, χ^2 was $\leq 1.5 \times 10^{-3}$ (see Table 4). Given the complexity of the fitting procedures and the quality of the data sets, we do not believe that the small variations in C (Table 2) are significant. The standard deviations report *precision*;

Table 2. Diffusion Coefficients for DODA in NDLDPE

T^a (°C)	$D_1 \times 10^9$ (cm^2 s^{-1})	$D_2 \times 10^9$ (cm^2 s^{-1})	C	χ^2 ($\times 10^5$)
24.5	2.0 ± 0.1	0.32 ± 0.07	0.24 ± 0.01	2.11
25.0	1.2 ± 0.2	0.42 ± 0.02	0.15 ± 0.06	5.65
35.5	8.9 ± 0.1	0.61 ± 0.01	0.15 ± 0.01	1.36
35.5	3.7 ± 0.1	0.56 ± 0.01	0.19 ± 0.01	6.30
45.5	10.4 ± 0.2	0.58 ± 0.01	0.19 ± 0.01	3.62
46.0	8.6 ± 0.1	0.63 ± 0.01	0.22 ± 0.01	2.64

[a] ±0.3 °C.

Table 3. Diffusion Coefficients for DMA in NDLDPE

T^a (°C)	$D \times 10^9$ (cm^2 s^{-1})	$\chi^2 \times 10^5$
25.0	6.5 ± 0.1	7.44
25.2	6.5 ± 0.1	8.16
35.0	14.6 ± 0.1	6.63
35.1	15.5 ± 0.1	4.13
45.5	37.4 ± 0.1	8.56
45.6	33.5 ± 0.1	12.0

[a] ±0.3 °C.

Table 4. Diffusion Coefficients for DMA (10^{-1} M Initial Concentration) in NDLDPE

T^a (°C)	$D \times 10^9$ (cm^2 s^{-1})	$\chi^2 \times 10^4$
25.2	3.8 ± 0.1	12
25.2	5.1 ± 0.1	15
25.1	4.6 ± 0.1	5.1
25.4	4.9 ± 0.1	15
35.4	11.2 ± 0.1	5.7
35.5	12.9 ± 0.1	5.3
35.5	12.8 ± 0.1	10
35.4	20.5 ± 0.1	3.7
45.7	31.6 ± 0.3	5.3
45.6	29.9 ± 0.1	2.6
45.5	22.6 ± 0.2	12

[a] ±0.3 °C.

Table 5. Activation Energies for DMA and DODA Diffusion in NDLDPE

DAA	E_{D1} (kcal mol^{-1})	E_{D2} (kcal mol^{-1})	D_{O1} (cm^2 s^{-1})	D_{O2} (cm^2 s^{-1})
DMA	15.7 ± 0.4		(2 ± 1) × 10^3	
	19 ± 5[a]		(1 ± 3) × 10^4 [a]	
	(15.1 ± 0.3)[b]			
DODA	16 ± 4	4 ± 1	(1 ± 7) × 10^3	(0.8 ± 1.7) × 10^3

[a] Ca. 10^{-1} M initial DMA concentration. [b] From ref 5a; using ODLDPE.

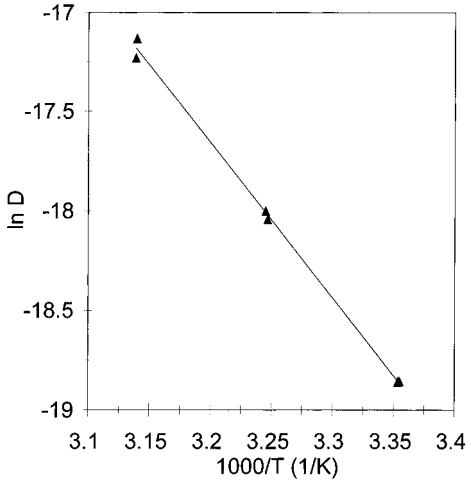

Figure 5. Arrhenius plot for DMA diffusion coefficients from experiments with ca. 10^{-3} M initial dopant concentrations.

the accuracy error limits (not calculated) should place all of the C within the range of one value, ca. 0.2.

$$D = D_0 \exp\left(\frac{-E_D}{RT}\right) \quad (4)$$

The E_D values (Table 5) were calculated from the slopes of Figures 5−7 assuming the diffusion coefficients follow an Arrhenius-type behavior (equation 4).[11b] D_0 values contain a very large error since the temperature range is small, the extrapolation of T^{-1} to ∞ is large,

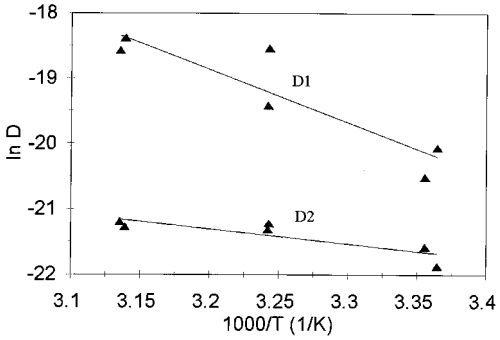

Figure 6. Arrhenius plots for faster and slower DODA diffusion coefficients with ca. 10^{-3} M initial dopant concentrations.

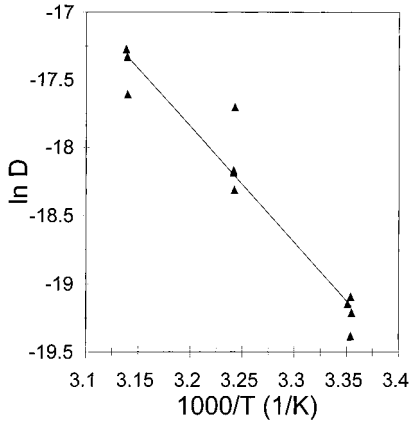

Figure 7. Arrhenius plot for DMA diffusion coefficients from experiments with ca. 10^{-1} M initial dopant concentrations.

and the precision of the individual D values has significant error limits (as shown by the differences between duplicate run values). The utility of the calculated D_0 values is limited, and they will not be interpreted here (although they are reasonable[11b]). Note, however, that the value of D_0 is about one order of magnitude higher for DMA experiments at the higher initial concentration than at the lower one. An increase in D_0 is an expected consequence of bulk plasticization (*vide infra*).

Discussion

Our previous investigations of the factors controlling the dynamics of diffusion of guest molecules in native polyethylene have followed two approaches. In the first, the diffusion coefficients and activation energies for diffusion of *three* DAAs (including DMA and DBA) were compared in *one* film (ODLDPE; 35% crystallinity and 0.917 g/cm^3 density at room temperature).[5a] In the second, the diffusion coefficients of *one* guest molecule, DMA, were compared in *five* films of differing physical characteristics (from 29 to 71% crystallinity and 0.916 to 0.945 g/cm^3 density).[6] These results, in combination with others employing native and modified polyethylene films, have revealed many of the important aspects of the polymer matrix that influence the diffusion of the DAA. However, they raise other very important mechanistic questions.

For instance, in ODLDPE at one temperature, the diffusion coefficient of the smaller DMA (molecular mass 121 and calculated van der Waals volume 128.7 Å^3 [14]) is larger than that of DBA (molecular mass 205 and calculated van der Waals volume 231.0 Å^3 [14]), as expected, but the activation energy of the smaller mol-

ecule, 15.1 kcal/mol, is somewhat *higher* than that of DBA, 13.4 kcal/mol.[5a] This contraintuitive observation must be tempered by the fact that the *accuracy* of the measurements probably brings the two values of E_D within the limits of experimental error. Regardless, the magnitudes of the E_D are much higher than expected on the basis of the energies associated with the various relaxation processes of polyethylene that should be instrumental in facilitating the movement of molecules locally between guest sites; thus, the flow activation energy, related to the motion of intertwined (reptating) segments of polymethylene chains,[15] is ca. 8 kcal/mol,[16] and even the highest energy (α) relaxation process, associated with the motion of chains at the surfaces of and in crystallites,[17] is no more than ca. 10 kcal/mol. On this basis, we conjectured that since the "widths" of the DAA aromatic rings are about twice the cross-sectional diameter of a methylene group, the coordinated motion of at least *two neighboring polymethylene chains* is required for a DAA molecule to hop between adjacent sites[18] and that such hopping is the rate-limiting step in the overall diffusion process.

Regardless, the similarity of the E_D values for DMA and DBA raises the possibility that DAA with longer alkyl chains might be able to *plasticize* their *local* environment, thereby facilitating their own diffusion. To test this possibility, we have compared the diffusional characteristics of DODA (molecular mass 597 and calculated van der Waals volume 708.4 Å^3 [14]) and the much smaller DMA in one polyethylene film, NDLDPE, at comparable, low (ca. 10^{-3} M) initial dopant concentrations where macroscopic film swelling and bulk plasticization should be unimportant. In addition, diffusion of DMA has been measured when its initial concentration in NDLDPE is increased to ca. 10^{-1} M (i.e., where bulk swelling and plasticization are expected to be consequential).

In all of the experiments with DMA and DBA in ODLDPE, the diffusional data could be fit to a classical model of Fickian diffusion by one diffusion coefficient.[5a] The same is true in experiments involving diffusion of DMA in four different low-density polyethylene films, *but not for the data sets in the high-density film* (BHDPE; 0.945 g/cm^3 density and 71% crystallinity).[6] There, the data could be fit only when a *second* diffusion process (and a second diffusion coefficient) was added to the model.

Unimodal distributions of stochastic diffusion are the norm in polymer films of polyethylene.[10,11] To the best of our knowledge, no other examples of *bimodal* distributions have been reported. In spite of this, it is reasonable to expect that even in cases where the diffusion is apparently unimodal, *it is phenomenologically bimodal* since guest molecules can reside in both amorphous and interfacial regions. Only if the dynamics of guest motion in the two regions are the same or if the DAA change positions between the two site types much more rapidly than they move to a film surface should it not be possible, at least in principle, to distinguish the modes of diffusion. Within this model, increasing the crystallinity and density of the host polyethylene allows the two diffusional processes of the relatively small guest molecule DMA to be distinguished.[6] Here, we have examined the diffusion of the much larger DODA in NDLDPE, a polyethylene of much lower crystallinity and density, to test further the model by determining whether the two modes of diffusion can be discerned again, and, more importantly, to gain insights concerning the environments in which the diffusional processes occur.

The Experimental Method. The method employed to obtain the diffusional data has been described previously.[5c,13] In the present cases, all of the necessary experimental conditions for its application are met: (1) the "receiving liquid", 2 N HCl, does not enter the polyethylene films; (2) DAA, the diffusing species, absorbs and emit weakly when in the liquid; (3) the diffusing molecules absorb and emit strongly when in the film; (4) the DAA molecules are dissolved and dispersed into the much larger volume of the receiving liquid when they leave the film. In fact, when condition 4 is met, condition 2 need not be since the volume of the film is less than 1% of the 3 mL liquid volume.

Normally, a large hydrophobic molecule like DODA, or even a smaller one like DMA, is not soluble in aqueous media. In this case, the very low pH of the liquid allows the aniline nitrogen atom to be protonated, creating a tertiary ammonium salt with sufficient solubility to be taken into the liquid at the concentrations employed. The total DODA concentration in the 2 N HCl at the end of a run (when diffusion from a film is complete) is $<10^{-5}$ M.

Diffusion of DMA. The values of D and E_D for DMA in NDLDPE and in ODLDPE are very similar and the activation energies are within experimental error. This correspondence was expected since the two polyethylenes were obtained as related materials from the same manufacturer and their crystalline contents are similar. Although the temperature bounds over which the data were collected, 15−34 °C for ODLDPE and 25−45.5 °C for NDLDPE, are not the same, they are far from any transitions, including those for formation of a glass at ca. −30 °C and for melting at ca. 120 °C.[19]

Since the diffusional processes of DMA in the two polyethylene films appear to be ostensibly the same, we assume that conclusions from the other DAA investigated in ODLDPE can be extrapolated to NDLDPE. In fact, there is very little difference among the values of D for DMA in the four low-density polyethylenes examined.[6]

The E_D value for DMA diffusion in NDLDPE from the higher dopant concentration experiments, 19 ± 5 kcal/mol, is within the experimental error of the other activation energies cited, but the error limits are symptomatic of the fact that the D values from individual runs could not be fit easily to equation 2 (or eq 1; Table 4). This indicates that the morphology of the films was altered significantly by the large amount of DMA initially localized in the amorphous and interfacial regions. As DMA diffused from the film, its morphology and the ability of the remaining DMA molecules to diffuse changed *during a run*.[20] Swelling and/or plasticization by the diffusing species does alter the dynamics of its motion in a film, but we have not quantified the effects as yet.

Diffusion of DODA. The diffusion of DODA in NDLDPE is much more complicated than that of DMA (Table 2). Each of the data sets could not be fit to eq 2, but a model in which two independent diffusion pathways are followed concurrently (eq 3) can. Phenomenologically, the model predicts that molecules of DODA experience different rate-limiting steps. We do not envision either pathway as a single energy barrier. Instead, there is a series of barriers associated with the movement of a molecule as it migrates among many host sites.[18]

Insights into the natures of the dual pathways come from the magnitudes of the D values at one temperature, the values of the associated E_D values, and the independent observation that diffusion of DMA in the *high-density* polyethylene film (BHDPE) also requires a dual pathway model; the data sets can be fit by eq 3, but not by eq 2.[6] In BHDPE at 25 °C, the ratio of the faster to slower D values, D_1/D_2, is about 20 and the *faster* diffusion pathway is followed by more than 80% of the DMA molecules. In NDLDPE at 25 °C, D_1/D_2 is 3−6 and ca. 80% of the DODA molecules follow the *slower* pathway. In low-density polyethylenes, like NDLDPE, the ratios of amorphous to interfacial volume fractions are smaller than in BHDPE; as the crystalline content increases, the interfacial fraction decreases more rapidly than the amorphous fraction.[6] On that basis, *we hypothesize that the faster DMA and DODA components are from molecules moving within the amorphous regions of a film and the slower components have their origin in diffusion within the interfacial regions*. Of course, molecules initially in one region will be able to migrate to the other, but the rate-limiting steps for macroscopic diffusion and the rates at which molecules enter and exit regions on a mesoscopic scale may have a very complex relationship.

Undoubtedly, there are other models that can be invoked to fit the data, but the most obvious ones are not as consistent with the information available. For example, molecules embedded nearer and farther from the surface of a film may diffuse differently. If they are the source of the dual diffusion coefficients, *all* of the DAA in *all* of the films should have produced similar results since the doping procedures were the same. We reject, also, any model involving diffusion in the crystalline portions since there is good evidence that molecules like the DAA cannot enter microcrystallites of polyethylene under the conditions of our experiments.[7,9] Similarly, the fact that dual diffusion coefficients are detected for more than one DAA[6] *and* the component contributions of the two pathways are virtually constant over the temperature ranges explored (Table 2) lead us to reject the possibility that one of the pathways is a result of microcrystallized DAA; like DODA in NDLDPE, DMA in high-density polyethylene requires two diffusion coefficients, but DMA is a liquid throughout the temperature range of the experiments. We assume that the amorphous/interfacial site model is correct.

In spite of the large differences in the sizes and masses of the diffusing molecules, the similarity between E_{D1} of DODA in NDLDPE and the E_D of the smaller DAA in ODLDPE was expected. Additionally, it is reasonable that the D values of DMA are only about four times the D_1 of DODA in NDLDPE. Since both DMA and DODA (in conformations with cylindrical shapes whose cross-sectional dimensions are near those of DMA) are within the "short molecule" limit (as defined by Moisan for ester diffusion in polyethylene[21]), the logarithms of their diffusion coefficients are predicted to vary linearly with molecular length[21] or with the logarithm of molecular mass.[22] Using either measure, our values of E_{D1} and D_1 seem appropriate.

However, the small magnitudes of D_2 and E_{D2}, from the slower component of DODA diffusion in NDLDPE, are intriguing. They do not correlate with literature values for diffusion of molecules of similar shape, size, and functionality in polyethylene.[4,5,11b] Assuming, as noted above, that the D_2 component derives from diffusion of DAA in the interfacial regions, its slowness may be due to anisotropy on a mesoscopic scale. DAA may be forced to move along the director axis of the nearly parallel chains of each interfacial domain. If so, their route from an interior site to a film surface will be longer than that followed by DAA migrating within the amorphous regions where chains are intertwined and not oriented, and diffusion is more tortuous. On the other hand, the energy required for movement of a DAA molecule like DODA, especially, should be lower in a sea of parallel polymethylene chains than in an entangled mass of them. Whether this energy difference is adequate to explain the enormous disparity between the two diffusional modes is unknown at present. Regardless, the fact that E_{D2} is only about 4 kcal/mol limits the nature of the interactions of the affected DODA molecules with their immediate environment. Local motions cannot depend critically upon flow activation or other parameters that are related to reptation of long segments of polymethylene chains. An attractive possibility that will require future experimental examination is that isolated DODA molecules do, indeed, plasticize their local environments.

Acknowledgment. We are pleased to acknowledge technical assistance from Dr. Donald Weber and Mr. William Craig. Dr. Oscar Zimerman and Mr. Liangde Lu are thanked for several helpful suggestions. We thank the National Science Foundation and the donors of Petroleum Research Fund, administered by the American Chemical Society, for their support of this research.

References and Notes

(1) (a) Axelson, D. E.; Levy, G. C.; Mandelkern, L. *Macromolecules* **1979**, *12*, 41. (b) Glenz, W.; Peterlin, A. *J. Macromol. Sci. Phys.* **1970**, *B4*, 473. (c) Hadley, D. W. In *Structures and Properties of Oriented Polymers*; Ward, I. M., Ed.; Wiley: London, 1975; Chapter 9. (d) Nordemeier, E.; Lanver, U.; Lechner, M. D. *Macromolecules* **1990**, *23*, 1072, 1077.

(2) Mandelkern, L. *Acc. Chem. Res.* **1990**, *23*, 380.

(3) Mutter, R.; Stille, W.; Strobl, G. R. *J. Polym. Sci., Polym. Phys. Edn.* **1993**, *31*, 99.

(4) (a) Jenkins, R. M.; Hammond, G. S.; Weiss, R. G. *J. Phys. Chem.* **1992**, *96*, 496. (b) He, Z.; Hammond, G. S.; Weiss, R. G. *Macromolecules* **1992**, *25*, 1569. (c) Naciri, J.; Weiss, R. G. *Macromolecules* **1986**, *19*, 1486. (d) Naciri, J.; He, Z.; Costantino, R. M; Lu, L.; Hammond, G. S.; Weiss, R. G. In *Multidimensional Spectroscopy of Polymers*; Urban, M. W., Provder, T., Eds.; American Chemical Society: Washington, DC, 1995; Chapter 25.

(5) (a) Lu, L.; Weiss, R. G. *Macromolecules* **1994**, *27*, 219. (b) Talhavini, M.; Atvars, T. D. Z.; Cui, C.; Weiss, R. G. *Polymer* **1996**, *37*, 4365. (c) Cui, C.; Naciri, J.; He, Z.; Jenkins, R. M.; Lu, L.; Ramesh, V.; Hammond, G. S.; Weiss, R. G. *Quim. Nova* **1993**, *16*, 578.

(6) Zimerman, O. E.; Cui, C.; Wang, X.; Atvars, T. D. Z.; Weiss, R. G. *Polymer*, in press.

(7) Phillips, P. J. *Chem. Rev.* **1990**, *90*, 425.

(8) Weiss, R. G.; Ramamurthy, V.; Hammond, G. S. *Acc. Chem. Res.* **1993**, *26*, 530.

(9) (a) Jang, Y. T.; Phillips, P. J.; Thulstrup, E. W. *Chem. Phys. Lett.* **1982**, *93*, 66. (b) Meirovitch, E. *J. Phys. Chem.* **1984**, *88*, 2629. (c) Radziszewski, J. G.; Michl, J. *J. Phys. Chem.* **1981**, *85*, 2934.

(10) Crank, J. *The Mathematics of Diffusion*; Oxford University Press: London, 1956; p 45.

(11) (a) Comyn, J. In *Polymer Permeability*; Comyn, J., Ed.; Elsevier: London, 1985; Chapter 1. (b) Moisan, J. Y. In *Polymer Permeability*; Comyn, J., Ed.; Elsevier: London, 1985; Chapter 4.

(12) Shirley, D. A.; Zietz, J. R.; Reedly, W. H. *J. Org. Chem.* **1953**, *18*, 378. Note the discrepancy between the literature and reported melting points. Our analyses demonstrate unambiguously that our material is DODA and is pure.

(13) He, Z.; Hammond, G. S.; Weiss, R. G. *Macromolecules* **1992**, *25*, 501.
(14) Bondi, A. *J. Phys. Chem.* **1964**, *68*, 441.
(15) Klein, J. *Nature* **1978**, *271*, 143.
(16) (a) Mendelson, R. A.; Bowles, W. A.; Finer, F. L. *J. Polym. Sci., Polym. Phys. Ed.* **1970**, *8*, 105. (b) Raju, V. R.; Smith, G. G.; Marin, G.; Knox, J. R.; Graessley, W. W. *J. Polym. Sci., Polym. Phys. Ed.* **1979**, *17*, 1183. (c) Pearson, D. S.; Ver Strate, G.; von Meerwall, E.; Schilling, F. C. *Macromolecules* **1987**, *20*, 1133.
(17) Boyer, R. F. *J. Polymer Sci.* **1966**, *C14*, 3.
(18) Vrentas, J. S.; Duda, J. L. *J. Polym. Sci., Polym. Phys. Ed.* **1977**, *15*, 403, 417, 441.
(19) Matsuoka, S. *Relaxation Phenomena in Polymers*; Hanser: Munich, Germany 1992.
(20) Hedenqvist, M.; Angelstok, A.; Edsberg, L.; Larsson, P. T.; Gedde, U. W. *Polymer* **1996**, *37*, 2887.
(21) Moisan, J. Y. *Eur. Polym. J.* **1981**, *17*, 857.
(22) Moisan, J. Y. *Eur. Polym. J.* **1980**, *16*, 979.

MA9615922